Murine Cell Lines Derived from *Pten* Null Prostate Cancer Show the Critical Role of PTEN in Hormone Refractory Prostate Cancer Development

Jing Jiao,[1] Shunyou Wang,[1] Rong Qiao,[1] Igor Vivanco,[1] Philip A. Watson,[2] Charles L. Sawyers,[2] and Hong Wu[1]

[1]Department of Molecular and Medical Pharmacology, University of California at Los Angeles, Los Angeles, California, and [2]Human Oncology and Pathogenesis Program, Memorial Sloan-Kettering Cancer Center, New York, New York

Abstract

***PTEN* mutations are among the most frequent genetic alterations found in human prostate cancers. Our previous works suggest that although precancerous lesions were found in *Pten* heterozygous mice, cancer progression and metastasis only happened when both alleles of *Pten* were deleted. To understand the molecular mechanisms underlying the role of PTEN in prostate cancer control, we generated two pairs of isogenic, androgen receptor (AR)–positive prostate epithelial lines from intact conditional *Pten* knock-out mice that are either heterozygous (PTEN-P2 and -P8) or homozygous (PTEN-CaP2 and PTEN-CaP8) for *Pten* deletion. Further characterization of these cells showed that loss of the second allele of *Pten* leads to increased anchorage-independent growth *in vitro* and tumorigenesis *in vivo* without obvious structural or numerical chromosome changes based on SKY karyotyping analysis. Despite no prior exposure to hormone ablation therapy, *Pten* null cells are tumorigenic in both male and female severe combined immunodeficiency mice. Furthermore, knocking down PTEN can convert the androgen-dependent Myc-CaP cell into androgen independence, suggesting that PTEN intrinsically controls androgen responsiveness, a critical step in the development of hormone refractory prostate cancer. Importantly, knocking down AR by shRNA in *Pten* null cells reverses androgen-independent growth *in vitro* and partially inhibited tumorigenesis *in vivo*, indicating that PTEN-controlled prostate tumorigenesis is AR dependent. These cell lines will serve as useful tools for understanding signaling pathways controlled by PTEN and elucidating the molecular mechanisms involved in hormone refractory prostate cancer formation.** [Cancer Res 2007;67(13):6083–91]

Introduction

Prostate cancer is the second leading cause of cancer-related death among North American men (1). Despite improved early detection and initial positive response to androgen ablation therapies, almost all patients eventually develop hormone refractory prostate cancer (HRPC). The molecular mechanisms leading to the progression of HRPC are still poorly understood (2), with proposed hypotheses ranging from gain of function mutations under hormone deprivation to intrinsic properties of certain prostate cancer cells (3).

Among genetic alterations frequently found in human prostate cancers, *PTEN* loss of function has been strongly implicated in prostate cancer development (4, 5). The etiologic role of PTEN in prostate tumorigenesis is further supported by studying animal models with prostate-specific deletion of its murine homologue, the *Pten* gene (6–8). In contrast to conventional heterozygous *Pten* deletion (6, 9, 10), conditional deletion of both alleles of *Pten* significantly reduces the latency of prostate intraepithelial neoplasia (PIN) lesion development and further progression to localized adenocarcinoma followed by metastasis (6–8). Therefore, the onset and progression of prostate cancer are PTEN dosage dependent (6). Similar to the majority of human prostate cancers, *Pten* null murine prostate cancer initially regress in response to androgen ablation therapy, but subsequently relapse and proliferate in the absence of androgens (7). Therefore, the *Pten* prostate cancer model (7) provides an ideal system for studying the mechanism of HRPC (11).

To our knowledge, the most well-studied human prostate cancer cell lines such as LNCaP (12), PC3 (13), and DU145 (14) are derived from late-stage cancer samples after hormone ablation therapy and therefore, are not ideal for studying the processes involved in HRPC. To circumvent this, we attempted to establish primary cell lines from intact *Pten* conditional knock-out mice (7). Here, we report the establishment and characterization of two pairs of isogenic cell lines and their usage to address (*a*) whether prostatic epithelial cells can acquire androgen independency without androgen deprivation and (*b*) the relationship between loss of PTEN and androgen-independent growth.

Materials and Methods

Establishment of primary cell lines from *Pten* prostate cancer model. Prostate cancer tissue was dissected from a 10-month intact $Pten^{loxp/loxp}$;*PB-Cre4*$^{+}$ mouse (7), minced, and digested with 0.5% type I collagenase (Invitrogen) using the same protocol as the generation of Myc-CaP line (15). After filtering through a 40-μm mesh, the fragments trapped by the mesh were plated in tissue culture dishes coated with type I collagen (BD Pharmingen). Several cell populations with distinct epithelial morphology were observed in the confluent monolayer developed from the tissue fragments. Cells with typical epithelial morphology were collected, and single cell was plated into each well of a 96-well plate. The PTEN-P2 and PTEN-P8 cell lines were independently established as spontaneously immortalized lines. The lines were maintained in DMEM supplemented with 10% fetal bovine serum (FBS; Omega Scientific), 25 μg/mL bovine pituitary extract, 5 μg/mL bovine insulin, and 6 ng/mL recombinant human epidermal growth factor (Sigma-Aldrich). The PTEN-CaP2 and PTEN-CaP8 were generated by infecting PTEN-P2 or PTEN-P8 cell

Note: Supplementary data for this article are available at Cancer Research Online (http://cancerres.aacrjournals.org/).

Requests for reprints: Hong Wu, Department of Molecular and Medical Pharmacology, University of California at Los Angeles School of Medicine, 650 CE Young Drive South, Los Angeles, CA 90095-1735. Phone: 310-825-5160; Fax: 310-267-0242; E-mail: hwu@mednet.ucla.edu.

doi:10.1158/0008-5472.CAN-06-4202

lines with Cre-retrovirus followed by 2 weeks of puromycin selection. Cells were genotyped by standard genomic PCR techniques, and the three primers used were 5′-TCCCAGAGTTCATACCAGGA-3′, 5′-GCAATGGCCAGTACTAGTGAAC-3′, and 5′-AATCTGTGCATGAAGGGAAC-3′.

Real-time PCR. Total RNAs from culture cells were extracted with RNeasy Micro kit (Qiagen). RNAs were reverse transcribed into cDNA with SuperScript III First-Strand Synthesis System for qRT-PCR (Invitrogen), and quantitative PCR was done in the iQ thermal cycler (Bio-Rad) using the iQ SYBR Green Supermix (Bio-Rad) and in triplicate. Results were analyzed by the relative quantification method and expressed as relative RNA levels. ΔCT was calculated by normalizing the threshold difference of certain gene x with glyceraldehyde-3-phosphate dehydrogenase. The relative RNA level was then calculated by normalizing the ΔCT to the least abundant RNA species, which was arbitrarily set to 15. The relative RNA level of gene x is thus equal to $15-\Delta CT(x)$. Primers for OAS2 and IFNB1 were from Superarray. All other PCR primers were synthesized by Operon Biotechnologies and designed for the mouse sequence unless otherwise specified. The following primer pairs were used: AR forward, 5′-AACCAACCAGATTCCTTTGC-3′, reverse, ATTAGTGAAGGACCGCCAAC-3′; CK5 forward, 5′-ACCTTCGAAACACCAAGCAC-3′, reverse, 5′-TTGGCACACTGCTTCTTGAC-3′; CK14 forward, 5′-GACTTCCGGACCAAGTTTGA-3′, reverse, 5′-CCTTGAGGCTCTCAATCTGC-3′; CK8 forward, 5′-ATCGAGATCACCACCTACCG-3′, reverse, 5′-TGAAGCCAGGGCTAGTGAGT-3′; CK18 forward, 5′-ACTCCGCAAGGTGGTAGATG-3′, reverse, 5′-GCCTCGATTTCTGTCTCCAG-3′; TAP63 forward, 5′-GAAGGCAGATGAAGACAGCA-3′, reverse, 5′-GGAAGTCATCTGGATTCCGT-3′; DNp63 forward, 5′-TCTGATGGCATTTGACCCTA-3′, reverse, 5′-TACCAACAGATGGGAAGCAA-3′; PSCA forward, 5′-GCTGCTACTCTGACCTGTGC-3′, reverse, 5′-TTCACAATCGGGCTATGGTA-3′; CgA forward, 5′-GGGAGCTGGAACATAAGCAG-3′, reverse, 5′-TGTCCTCCCATTCTCTGGAC-3′; Syph forward, 5′-CTTTGTGAAGGTGCTGCAAT, reverse, 5′-GTCTTGTTGGCACAATCCAC-3′; Probasin forward, 5′-ATCATCCTTCTGCTCACACTGCATG-3′, reverse, 5′-ACAGTTGTCCGTGTCCATGATACGC-3′; OAS1 forward, 5′-TGGAAAGAAGAGGTCCTGGA-3′, reverse, 5′-ACGGTGCCATTCCCAAAGCA-3′.

Western analysis. Protein lysates were prepared from confluent cells by adding radioimmunoprecipitation assay buffer as described (16). Protein lysate (50 μg) was resolved on SDS-PAGE followed by Western blot analysis using anti-PTEN (9552, Cell Signaling Technologies), AR (N-20, Santa Cruz Biotechnology), P-AKT (9271, Cell Signaling Technologies), total AKT (9272, Cell Signaling Technologies), Nkx3.1 (sc-15022, Santa Cruz Biotechnology), Cre (MAB3120, Chemicon), p21(sc-471, Santa Cruz Biotechnology), p27 (sc-1641, Santa Cruz Biotechnology), E-cadherin (610181, BD Biosciences), and β-actin (5441, Sigma) antibodies, respectively.

Spectral karyotyping analysis. Cells were harvested after mitotic arrest with colcemid (0.05 μg/mL) for 2 h. Hypotonization was done with 0.075 mol/L KCl, and a 3:1 mixture of methanol and glacial acetic acid was used for fixation. Slides underwent SKY [Applied Spectral Imaging (ASI)] hybridization, posthybridization, and analyses following ASI's recommended procedures. The probe cocktail contained 20 differentially labeled chromosome-specific painting probes and Cot-1 blocking DNA. Image acquisition was done using a SD300 Spectracube system (ASI) mounted in an Olympus BX60 microscope with a custom-designed optical filter (SKY-1, Chroma Technology). Ploidy was defined by the chromosome count for each metaphase and was noted by a specific range. Chromosomal gain and/or loss were determined by the average of the observed copy number ± 25%. Any structural abnormality seen in two or more cells was considered clonal. On average, 15 cells per cell line were analyzed.

***In vitro* cell growth assay.** For the Casodex treatment experiment, cells (5×10^4 cells per plate) were plated in medium containing 10% FBS with or without 10 μmol/L Casodex for 3 days. To determine cell growth in charcoal-stripped serum (CSS) medium, cells were seeded into six-well plates at 5×10^4 cells per well in the maintenance media containing 10% FBS for 16 h. Plates were then cultured in 4% CSS medium for 5 or 6 days. Cell proliferation was determined by trypsinizing and counting live cells using trypan blue dye exclusion method every 2 days. Each cell line was assayed in triplicate, and the assay was repeated twice.

Soft agar colony formation assay. Cells were plated at a density of 10,000 cells per plate in 0.3% agar on 6-cm tissue culture dishes coated with 0.6% agar in DMEM growth medium. Twenty days after plating, plates were stained with 0.5 mL 0.005% crystal violet. Colonies were counted under a light microscope (4×). Only colonies larger than 0.1 mm diameter were included.

Viral transduction. Androgen receptor (AR) knockdown was achieved by infecting PTEN-CaP2 and PTEN-CaP8 cells with pSIREN-RetroQ-DsRed (pSRQ-R, Clontech Laboratories, Inc.) retrovirus expressing AR-specific short hairpin RNA (shRNA).

AR shRNA-1 primer: 5′-GATCCGCGATTGTACCATTGATAAATTCAAGAGA TTTATCAATGGTACAATCGTTTTTTACGCGTG-3′ and 5′-AATTCACGCGTAAAAAACGATTGTACCATTGATAAATCTCTTGAATTTATCAATGGTACAATCGCG-3′. AR shRNA-2 primer: 5′-GATCCG AGAATCGCGACTACTACAATTCAAGAGATTGTAGTAGTCGCGATTCTTTTTTTACGCGTG-3′ and 5′-AATTCACGCGTAAAAAAAGAATCGCGACTACTACAATCTCTTGAATTGTAGTAGTCGCGATTCTCG-3′. The annealed oligos were cloned into the *Bam*HI-*Eco*RI site of pSRQ-R, and positive clones were confirmed by sequencing. pSRQ-R/AR–shRNA or control vector containing control shRNA (Clontech) and packaging plasmid were transfected into 293T packaging cells individually, and the collected retrovirus was used to infect PTEN-CaP2 and PTEN-CaP8 cells. Cre recombinase virus was made by transfecting pMSCV-puro-Cre and ecotropic packaging plasmid into 293T cells. To knockdown PTEN expression in Myc-CaP, cells were infected with lentivirus expressing either GFP or PTEN-specific shRNA (17).

***In vivo* tumor formation study.** Cells (1×10^6) were first mixed with Matrigel (BD Bioscience) solution at a ratio of 1:1 and then inoculated s.c. into severe combined immunodeficiency (SCID) mice (≤3 months of age). Tumor formation was monitored for 3 to 8 weeks. Tumor size was determined by caliper measurements, and tumor volume was calculated by a rational ellipse formula ($m_1 \times m_1 \times m_2 \times 0.5236$, where m_1 is the short axis and m_2 is the long axis). To examine the role of PTEN in androgen-independent tumor formation, 72 h after viral infection, infected Myc-CaP cells were replated in CSS medium for an additional 2 days, and then cells (2×10^5) were injected into flanks of precastrated SCID or intact SCID mice.

Histology and immunohistochemical analysis. Histologic and immunochemical analyses were done as described (16). Briefly, formalin-fixed and paraffin-embedded (PFPE) sections were stained with H&E or specific antibodies to AR (N-20, Santa Cruz Biotechnology) and Ki67 (VP-RM04, Vector Laboratories) as described (7). For immunofluorescence staining, pretreated sections were first blocked and then incubated with monoclonal antibody against CK8 (MMS162-P, Covance), SMA (M0851, DAKO) at room temperature for 30 min, followed by incubation with Alexa Fluor-594 goat anti-mouse immunoglobulin G (IgG; H+L; 1:1,000; Molecular Probes). Sections were counterstained with 4′,6-diamidino-2-phenylindole in mounting medium (Vector Laboratories) and analyzed by fluorescence microscopy.

Statistical analysis. All data were presented as means ± SE. Statistical calculations were done with Microsoft Excel analysis tools. Differences between individual groups were analyzed by paired t test. P values of <0.05 were considered statistically significant.

Results

Establishment and characterization of two isogenic prostatic epithelial cell lines from the *Pten* conditional knock-out model. To facilitate our investigation of the molecular mechanisms underlying PTEN-controlled prostate tumorigenesis, we isolated primary prostatic cells from an intact $Pten^{loxp/loxp};PB\text{-}Cre4^{+}$ mouse using the same protocol as the generation of Myc-CaP line (15). After serial passages and spontaneous immortalization (see Materials and Methods for details), several clonally derived cell lines were established and from which two lines, named PTEN-P2 and PTEN-P8, were further characterized and studied herein.

Our initial genotyping analysis suggested that PTEN-P2 and PTEN-P8 were heterozygous for *Pten* deletion, although the Cre

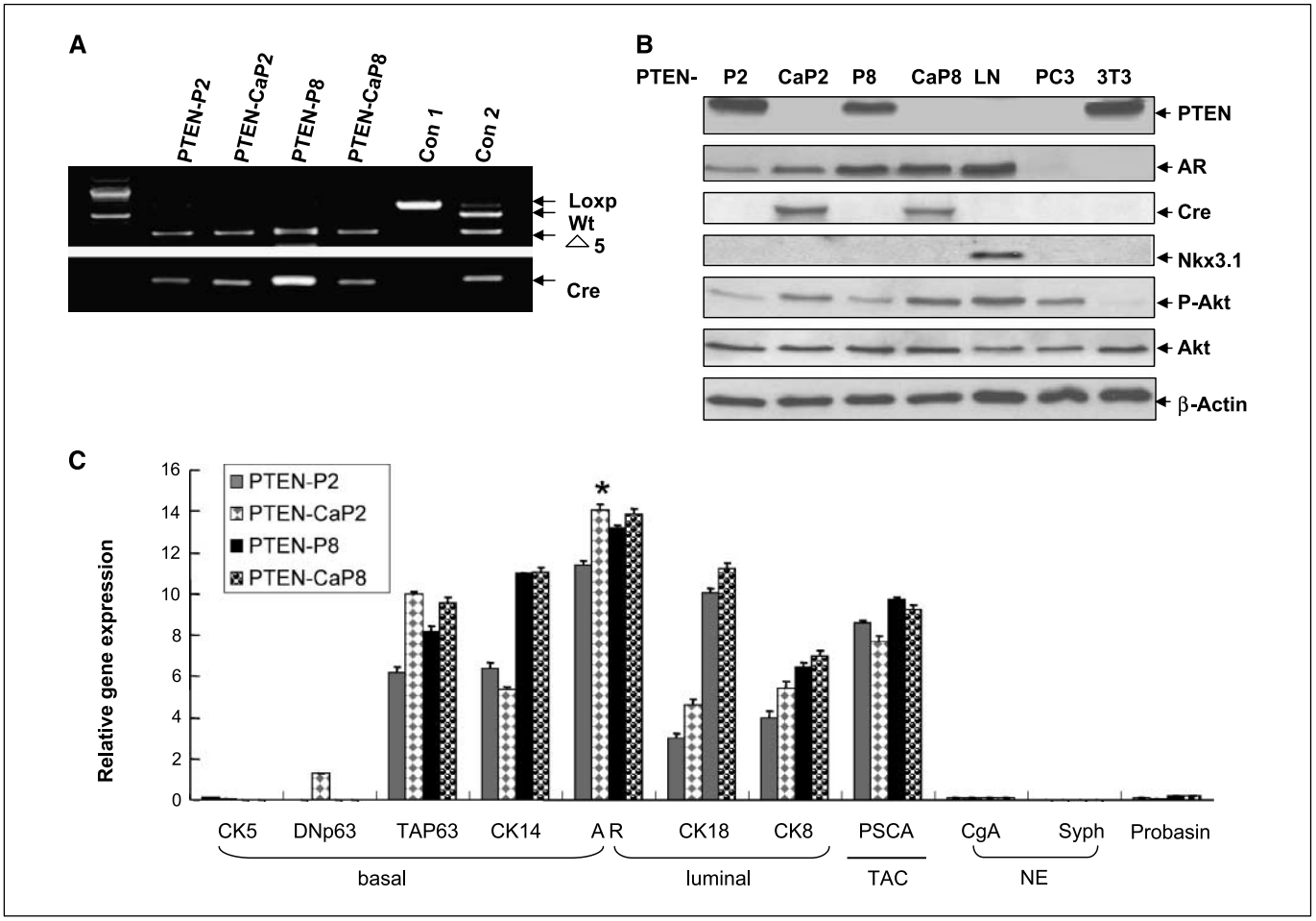

Figure 1. Characterization of two pairs of novel prostate cell line derived from *Pten* conditional knock-out mice. *A,* PCR-based genotyping analysis of established cell lines. Genomic DNA from cells (*lanes 1–4*) or mouse tails (*lanes 5* and *6*) were extracted. PCR analysis showed that PTEN-P2 and PTEN-P8 are Lox/△5; Cre+, PTEN-CaP2, and PTEN-CaP8 are Δ5/Δ5;Cre+. Con1 and Con2 are loxp/loxp and loxp/+;Cre+ controls for genotyping. *B,* Western blot analyses of PTEN, AR, Cre, Nkx3.1, P-AKT, Akt expression in the established cell lines (PTEN-P2, PTEN-CaP2, PTEN-P8, PTEN-CaP8), and controls (LNCaP, PC3, NIH3T3). β-Actin was used as a loading control. *C,* real-time PCR analysis of phenotypic marker for the established prostate cell lines. These markers are associated with the neuroendocrine (*NE*) cells or the basal or luminal cells of the prostate. RNA preparation, real-time PCR conditions, product length, and primer sequences are described in Materials and Methods. *CK,* cytokeratin; *CgA,* chromogranin A; *Syph,* synaptophysin. *Columns,* mean; *bars,* SD; *, $P < 0.05$.

transgene could be easily detected in both lines (Fig. 1*A, lanes 1* and *3*). To rule out possible contamination, two additional rounds of subcloning were done, which further confirmed the heterozygous status of these two lines (data not shown). The incomplete deletion of *Pten* loxp alleles led us to further investigate the Cre transgene expression, which is under the control of a modified rat probasin promoter (18). Western blot analysis showed very low to undetectable Cre protein expression (Fig. 1*B, lanes 1* and *3*) and quantitative reverse transcription-PCR (Q-RT-PCR) analysis confirmed significant down-regulation of the endogenous probasin gene in both cell lines (Fig. 1*C*). Our recent finding showed that probasin is positively regulated by PTEN (16) through NKX3.1 (19): in the absence of PTEN, NKX3.1 expression as well as its downstream target genes, including probasin, are significantly down-regulated to undetectable levels in both human and murine prostate cancer tissues. Consistent with our recent finding (16), Western blot analysis showed very low to undetectable Nkx3.1 expression in both PTEN-P2 and PTEN-P8 lines (Fig. 1*B*). *Cre* expression, on the other hand, was significantly enhanced when a NKX3.1-expressing vector was transfected into these cells (Supplementary Fig. S1*A*).

We then infected PTEN-P2 and PTEN-P8 lines with a retrovirus carrying Cre and puromycin-resistant cassette and the resulting isogenic lines, PTEN-CaP2 and PTEN-CaP8 were generated after 2 weeks of drug selection. PCR-based genotyping and Western analysis showed that PTEN-CaP2 and PTEN-CaP8 had indeed lost the second $Pten^{loxp}$ allele and are null for PTEN function, as evident by the loss of PTEN protein expression and increased P-AKT levels (Fig. 1*A* and *B, lanes 2* and *4*). Interestingly, deletion of the second allele of *Pten* led to increased AR expression in the PTEN-CaP2 cells (comparing AR levels in Fig. 1*B, lanes 1* and *2*, and quantified in Supplementary Fig. S1*B*), consistent with our previous finding that PTEN serves as a negative regulator for AR expression (16).

To determine the cellular origin of these established cell lines, we did Q-RT-PCR analysis using primers corresponding to phenotypic markers for the major cell types in the prostate epithelium. As shown in Fig. 1*C*, all lines coexpress both basal (CK14, AR) and luminal cell (CK8/CK18, AR) but not neuroendocrine markers (Fig. 1*C*). Furthermore, PSCA, a marker that represents an intermediate stage between basal and luminal cells, the transient amplified cell population (20), is also highly expressed in all four cell lines (Fig. 1*C*). Taken together, these results suggest that the

parental PTEN-P2 and P8 lines were derived from epithelial cells and display similar expression patterns with the transient amplified cells (20).

Loss of the second allele of *Pten* does not cause global chromosomal alterations. Recent findings (21) have shown a novel nuclear function for PTEN in controlling chromosomal integrity. Chromosomal aberrations have previously been linked to the progression of prostate cancer (22). To examine whether there were any chromosome alterations between the isogenic prostate cells, we did karyotyping analyses using a combination of SKY and G-banding tests (Fig. 2). As summarized in Supplementary Table S1, our study revealed several structural and numerical alterations in each pair: PTEN-P2 and PTEN-CaP2 (Supplementary Fig. S2) contained near-tetraploid chromosome number, with 65 to 84 chromosomes in PTEN-P2 and 76 to 80 chromosomes in PTEN-CaP2, respectively; PTEN-P8 and PTEN-CaP8 had near 6N chromosomes with 113 to 125 chromosomes in PTEN-P8 and 115 to 129 chromosomes in PTEN-CaP8. Importantly, loss of the second allele of *Pten* did not cause further global structural or numerical changes under our *in vitro* culture conditions, at least within the sensitivities offered by SKY and G-banding analyses. Interestingly, all of the lines analyzed share several common chromosomal alterations that are highlighted in Supplementary Table S1, including del(7)C-F, +10, and a heteromorphous chromosome 8 with a very small centromere, which may either support their common origin or reflect basic genetic alterations required for immortalization of epithelial cells (23). Significantly, loss of the Y chromosome, which is one of the most frequent cytogenic changes observed in human sporadic prostate tumors (22), was observed in PTEN-P8 and PTEN-CaP8.

PTEN loss leads to increased anchorage-independent growth *in vitro* and increased tumorigenic potential *in vivo*. As a tumor suppressor, PTEN loss is often associated with a gain of transformation potential (24) as PTEN negatively regulates cell cycle progression, cell migration, and cell survival (25). To determine whether *Pten* loss of heterozygosity leads to enhanced transformation potential, soft agar assay was employed to examine the colony-forming efficiency of *Pten* null cells. After 20 days in culture, colonies were photographed and counted. PTEN-CaP2 and PTEN-CaP8 cells formed 5- and 2.5-fold more colonies compared with their parental heterozygous cells, respectively (Fig. 3*A, left*). In addition, the sizes of *Pten* null colonies were generally larger than those of heterozygous ones (Fig. 3*A, right*). PTEN-CaP2 and PTEN-CaP8 cells also expressed decreased levels of the G_1 cell cycle inhibitor p27, as compared with their isogenic heterozygous pairs (Fig. 3*B*). Interestedly, complete loss of PTEN also caused decreased E-cadherin expression (Fig. 3*B*), a molecule critically important for cell-cell adhesion and tumor invasion (26).

Studies from our group and others showed that PTEN dosage plays a critical role in determining both the onset and progression of prostate cancer (6–10). To examine whether the cell lines we generated could mimic the biological differences between *Pten* heterozygous and homozygous mutants *in vivo*, we next checked their tumorigenic potentials in immune incompetent SCID mice. Equal number of cells (1×10^6) was injected s.c. into the flank of male SCID mice, and tumor growth was monitored on a daily basis. Both *Pten* null lines (PTEN-CaP2 and PTEN-CaP8) were tumorigenic with a latency of 3 weeks. However, no tumor formation could be detected when the same number of *Pten* heterozygous cells (PTEN-P2 and PTEN-P8) were inoculated and followed up to 4 months (Fig. 3*C*), suggesting that the dosage effect of PTEN in tumorigenesis control can be recapitulated in these isogenic lines. Histologic analysis indicated that all xenograft tumors maintained AR expression and were positive for the luminal epithelial marker CK8 but not for the mesenchymal marker smooth muscle actin (SMA; Fig. 3*D*). Consistent with our Q-RT-PCR result, no neuroendocrine marker expression could be detected (data not shown).

Loss of PTEN promotes androgen-independent growth. Similar to human prostate cancers, *Pten* null murine prostate cancers do progress to HRPC after castration (7). To understand whether HRPC development requires additional genetic changes under low androgen levels, we tested the likelihood of the

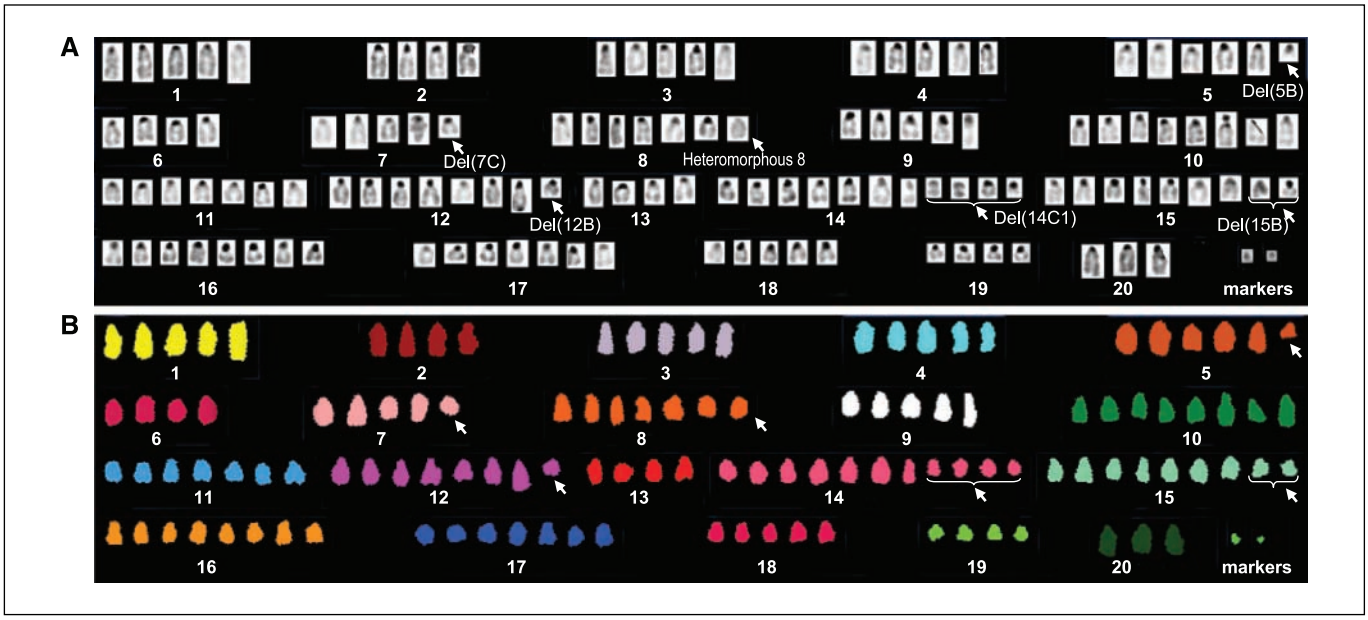

Figure 2. Representative karyotype of the PTEN-CaP8 cell line. Sequential G-banding (*A*) and SKY (*B*) analysis were done on metaphase preparations derived from PTEN-CaP8 cells. The chromosomal number is variable, but near 6N.

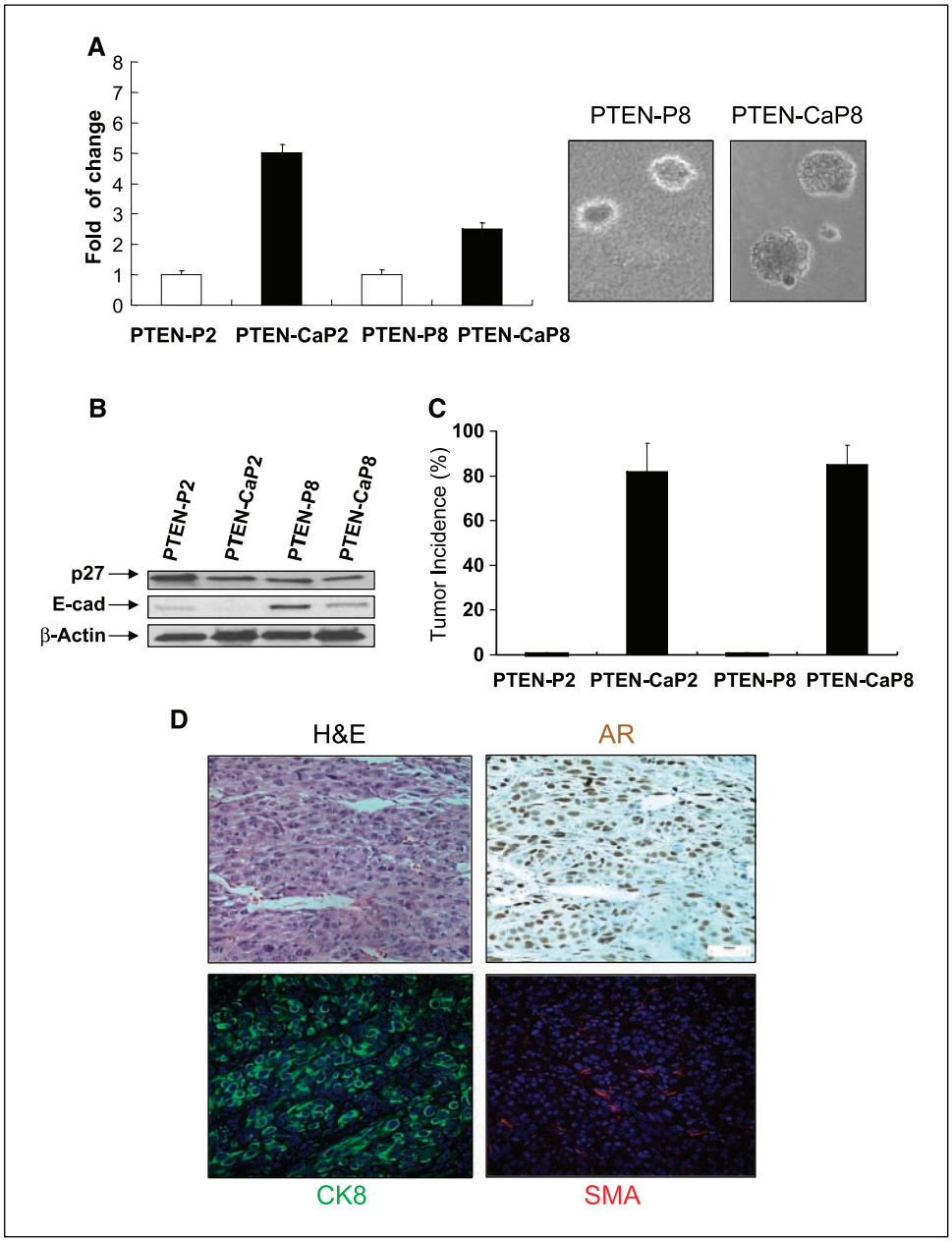

Figure 3. Loss of Pten increases anchorage-independent growth properties *in vitro* and promotes tumorigenesis *in vivo*. *A, left,* fold differences in number of colony formation in soft agar from *Pten* null prostate cells (PTEN-CaP2, PTEN-CaP8) relative to their corresponding isogenic pair (PTEN-P2, PTEN-P8); *right,* a representative picture showing the colony size difference. *B,* Western blot analysis showed that PTEN-CaP2 and PTEN-CaP8 had decreased p27, and E-cadherin expressions compared with its corresponding heterozygous control line PTEN-P2 and PTEN-P8. *C,* equal number of PTEN-P2, PTEN-CaP2 and PTEN-P8, PTEN-CaP8 cells were inoculated s.c. into male SCID mice ($n \geq 6$), and tumor incidences at 60 days were compared. *D,* consecutive sections from a PTEN-CaP8 tumor were stained with antibodies against AR, cytokeratin 8, and smooth muscle actin. *Bar,* 50 μm.

androgen-independent growth and tumor-forming potential of these cell lines that have never been exposed to such a selective pressure.

We first examined the cell growth property in the presence of androgen antagonist Casodex, a potent, nonsteroidal antiandrogen drug that has been shown to have robust inhibitory effects on the growth of human prostate tumor cell lines, including the androgen-dependent cell line LNCaP (27). Consistent with previous reports (27), Casodex efficiently inhibited LNCaP cell growth but had little effect on the PTEN-CaP2 and PTEN-CaP8 lines we generated in this study (Fig. 4*A*), indicating that the growth properties of these cell lines are not significantly changed with the addition of Casodex. Additionally, both PTEN-CaP2 and PTEN-CaP8 remained proliferative in the CSS medium (Supplementary Fig. S3).

We then examined the tumor formation *in vivo* in female SCID mice. Remarkably, both PTEN-CaP2 and PTEN-CaP8 could form tumors in female SCID mice with similar frequency and latency as in males (Fig. 4*B*). Histologic examination showed no detectable difference in tumors formed by each cell line in either female or male SCID mice. Ki67 index further confirmed similar proliferation potentials of xenograft tumors generated in both male and female recipient mice (Fig. 4*C*; Supplementary Fig. S4).

To further explore the relationship between loss of PTEN and androgen independence, we first compared the PTEN-CaP lines with the Myc-CaP line we generated recently (15). Although established using an identical culture condition, Myc-CaP cells cannot grow in the androgen-ablated environment *in vivo* (15). Therefore, the androgen-independent nature of PTEN-CaP cells is unlikely due to the in vitro culture procedure. Interestingly, we did not find del(7)C-F, +10 chromosome abnormalities in Myc-CaP (data not shown) as what we have observed in PTEN-CaP2 and PTEN-CaP8 lines. Whether these chromosome abnormalities play a

role in the development of androgen independence is an open question and deserves further investigation.

To further examine whether loss of PTEN plays an intrinsic role in androgen independence, we accessed the impact of PTEN loss on the androgen responsiveness of Myc-CaP cells. Significantly, when infected by a lentivirus-carrying PTEN shRNA (17), Myc-CaP/PTEN-shRNA cells, but not cells infected with empty vector (Fig. 5*A*), became tumorigenic on both precastrated or intact SCID male mice (Fig. 5*B*). Taken together, these data suggest that PTEN plays a critical role in determining the androgen-independent growth potential of prostatic epithelial cells.

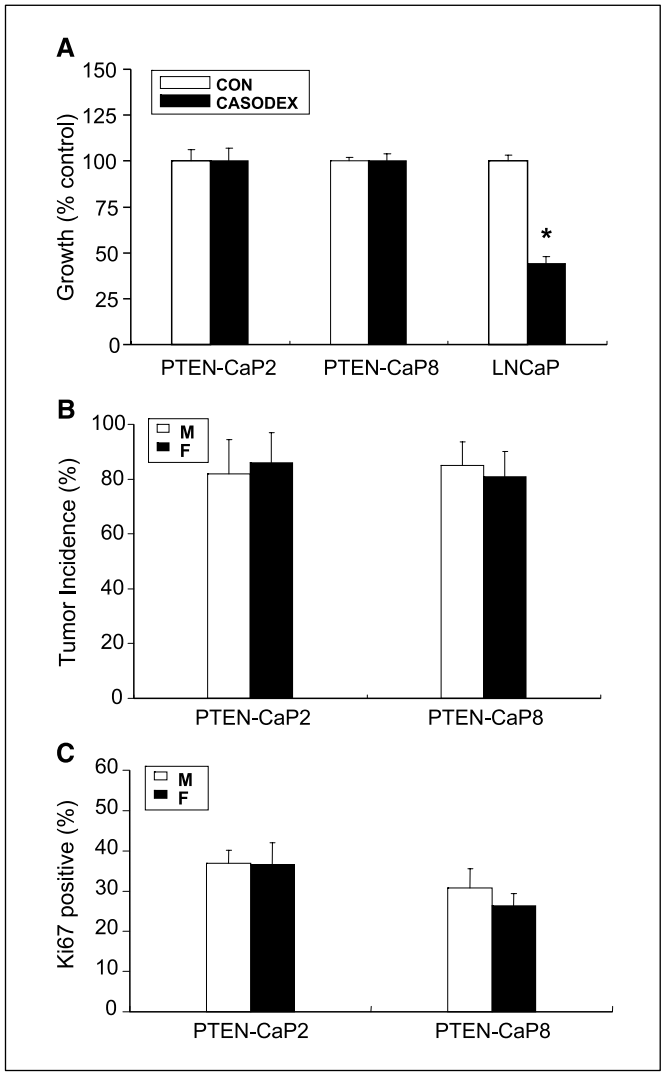

Figure 4. PTEN-CaP2 and PTEN-CaP8 are resistant to antiandrogen treatment *in vitro* and are tumorigenic *in vivo* in both male and female SCID mice. *A*, PTEN-CaP2 and PTEN-CaP8 are resistant to antiandrogen treatment. A total of 5×10^4 cells per well were plated in a six-well plate in triplicate containing 10% FBS DMEM maintenance medium with or without 10 μmol/L Casodex for 3 d. Live cell numbers were counted using trypan blue dye exclusion method. For each cell line, Casodex-treated cell growth is expressed as the percentage of cell numbers in relation to control DMSO-treated cells (100% growth). *Columns,* mean; *bars,* SD; *, $P < 0.05$. *B,* equal number (1×10^6) of PTEN-CaP2 and PTEN-CaP8 cells were inoculated s.c. into either male or female SCID mice ($n \geq 6$), and tumor incidences at 60 d were compared. Experiments were done twice, each with six animals per cohort. *C,* Ki67 index of tumors from female and male SCID mice. Consecutive sections were stained with antibodies against Ki67, and percent of Ki67+ cells were quantified.

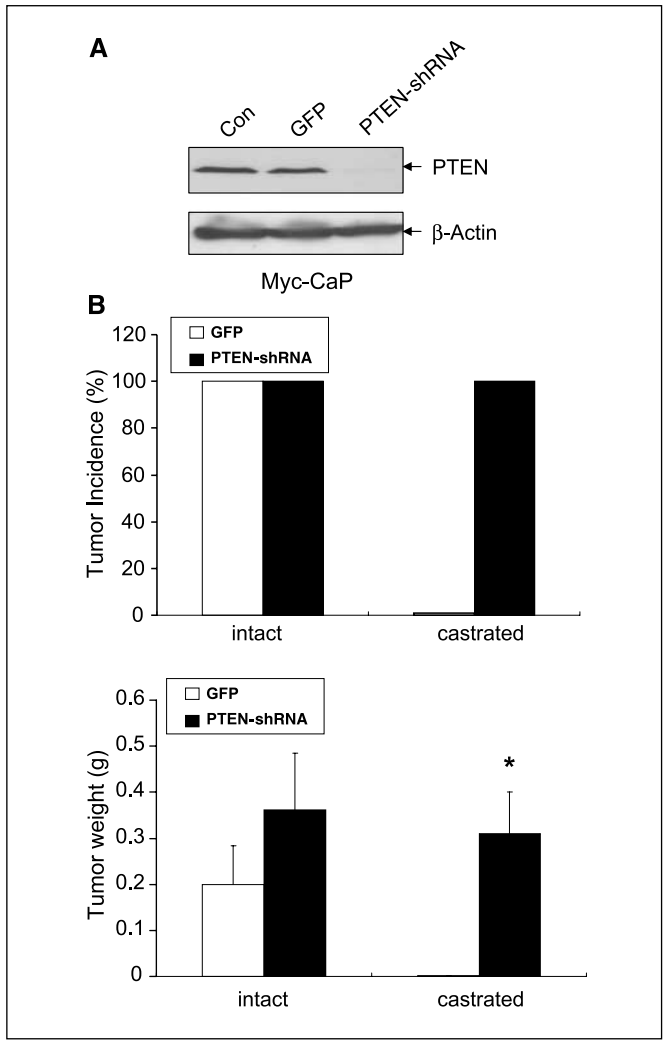

Figure 5. Knocking down PTEN in Myc-CaP cell is sufficient to change its androgen dependency. *A,* Myc-CaP cells were lentivirally infected with PTEN-targeted shRNA (*PTEN-shRNA*) or control virus containing GFP (*GFP*). Seventy-two hours after infection, cells were split into CSS medium for an additional 2 d. Lysates were made and analyzed by immunoblot with the indicated antibodies. The remaining cells were used for s.c. injection. *B,* 2×10^5 infected Myc-CaP (GFP) and Myc-CaP (PTEN-shRNA) were injected s.c. into the flanks of either precastrated SCID ($n = 4$) or intact SCID mice ($n = 4$). Tumors were harvested 21 d after inoculation. *Top,* tumor incidence difference 21 d after inoculation. *Bottom,* tumor weight differences among these groups. *Columns,* mean; *bars,* SD; *, $P < 0.05$.

AR is required for PTEN-controlled HRPC. Loss of PTEN and enhanced AR activity represent two common features of human prostate cancer, especially in HRPC (28). Unfortunately, among various prostate cancer cell lines, PC3 is null for both PTEN and AR (13), DU145 expresses PTEN but has AR loss (14), and LNCaP has mutated AR and PTEN loss (12). The *Pten* null prostatic epithelial cell lines we generated are AR positive without detectable mutations in the AR coding region (data not shown) and, therefore, can be used to address the relationship between PTEN loss and enhanced AR function. To evaluate the functional significance of AR in PTEN-controlled androgen-independent growth, we used AR shRNA to knockdown endogenous AR expression. Several short hairpins were generated corresponding to three different AR coding regions (29), and after initial analysis, two that showed most significant inhibitory effect were chosen for further functional

studies. As shown in Fig. 6*A*, the endogenous AR expression in PTEN-CaP2 and PTEN-CaP8 cells was reduced to almost undetectable levels upon shRNA-1 treatment, but shRNA-2 had less effect. At the same time, the G_1 cell cycle inhibitors p21 and p27 levels were significantly increased (Fig. 6*A*).

A growing body of evidence suggests that siRNA could generate off-target effects through different mechanisms (30–32). To exclude the potential effects of nonspecific IFN response by siRNA, we assessed the induction of 2′-5′oligoadenylate synthetase (OSA1), 2′-5′ oligoadenylate synthetase 2 (OAS2), and IFNβ1 (IFNB1), three classic IFN target genes. As shown in Fig. 6*B*, no significant differences in *OSA1, OAS2*, as well as *IFNB1* mRNA levels were detected when we compared with cells bearing control shRNA and AR shRNA-1 (Fig. 6*B*), indicating that the effect of AR shRNA was not mediated by general IFNβ response.

To further measure the biological effects of AR knockdown in *Pten* null cells, we first compared cell growth properties with control shRNA or AR shRNA-1 in androgen-ablated conditions. As shown in Fig. 6*C*, cell proliferation rates were significantly reduced in both PTEN-CaP2 and PTEN-CaP8 cells infected by AR shRNA-1, suggesting that AR plays an essential role in the cell cycle progression of *Pten* null prostatic epithelial cells. Importantly, AR knockdown significantly impaired the *in vivo* tumorigenic potentials of *Pten* null cells in female SCID mice (Fig. 6*D*). Taken together, our results indicate that AR is required for PTEN-controlled androgen-independent prostate tumorigenesis.

Discussion

One major obstacle to exploring the mechanisms underlying HRPC progression is the shortage of good model systems, either *in vivo* or *in vitro*, that can truly reflect human prostate cancer progression. The *Pten* murine prostate cancer model provides a valuable resource for studying the mechanism of HRPC (7). Here we report the characterization of two pairs of isogenic prostate cell lines established from the *Pten* null prostate cancer model. These

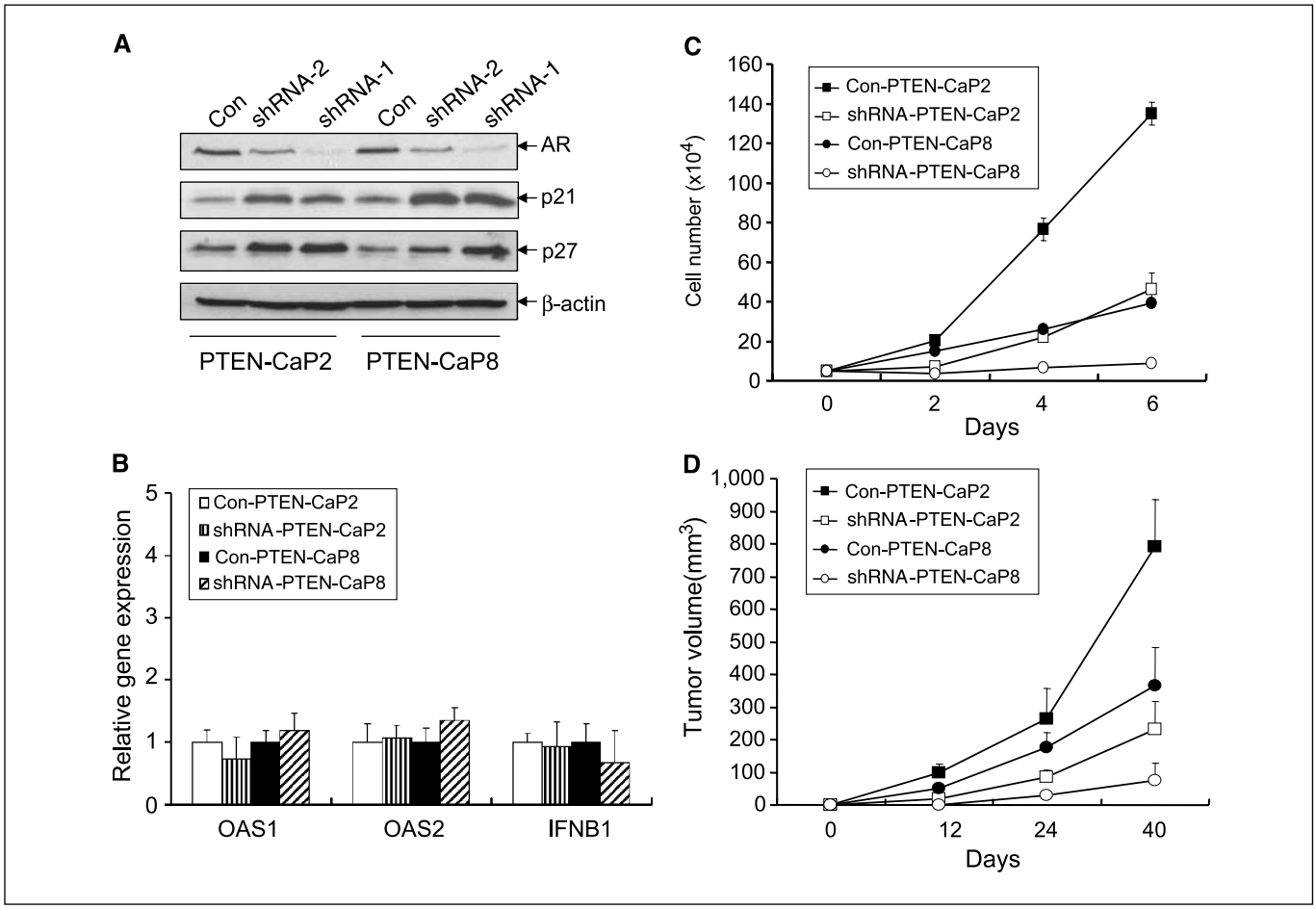

Figure 6. AR is required for PTEN-controlled androgen-independent tumorigenesis. *A,* knockdown AR expression caused a significant increased in p21 and p27 expression. PTEN-CaP2 and PTEN-CaP8 were retrovirally infected with AR-specific shRNAs (*shRNA-1* or *shRNA-2*) or control shRNA (*Con*). Seventy-two hours after infection, cells were harvested, and lysates were analyzed by immunoblotting with the indicated antibodies. *B,* AR knockdown in PTEN-CaP2 and PTEN-CaP8 does not induce significant IFN response. Seventy-two hours after AR-shRNA-1 or control-shRNA infection, infected PTEN-CaP2 and PTEN-CaP8 from (*A*) were seeded in CSS medium for additional 2 d. The OAS1, OAS2, IFNB gene induction was measured by quantitative real-time RT-PCR and presented as relative fold of change. *C,* AR shRNA leads to significantly decreased growth rates in PTEN-CaP2 and PTEN-CaP8 cells. Seventy-two hours after AR-shRNA or control-shRNA infection, infected PTEN-CaP2 and PTEN-CaP8 from (*A*) were seeded at 5×10^4 per well in six wells in triplicate containing CSS medium, and cell numbers were counted every 2 d. *Columns,* mean; *bars,* SD. *D,* AR knockdown impairs androgen-independent tumor growth. Con-PTEN-CaP2, AR-shRNA-PTEN-CaP2 and Con-PTEN-CaP8, AR-shRNA-PTEN-CaP8 from (*A*) were injected s.c. into female SCID mice ($n = 6$), and tumor volume was followed over the indicated time periods. *Columns,* mean; *bars,* SD.

murine prostate cancer cell lines not only mimic the biological difference between *Pten* heterozygous and homozygous mutants *in vivo*, but also provide the molecular insight into the critical role of PTEN in tumorigenesis and androgen responsiveness. Loss of PTEN enables cells to acquire transforming abilities without a significant change in global chromosome structure. Furthermore, loss of PTEN promotes androgen-independent growth *in vitro* and *in vivo*. Knockdown of PTEN expression, on the other hand, is sufficient to convert androgen-dependent Myc-CaP cells to androgen-independent growth, indicating PTEN's intrinsic role in regulating androgen-dependent growth. Using a shRNA approach, our study further shows the critical role of AR in PTEN-controlled androgen-independent tumorigenesis. Collectively, the murine cell lines established from our study can be used as research tools and may provide a unique opportunity for exploring both the molecular mechanism underlying HRPC and the development of new targeted therapies.

One interesting observation we made was that the two original spontaneously immortalized lines are *Pten* heterozygous, although the mouse from which the cell lines were generated was clearly $Pten^{loxp/loxp};PBCre4^{+}$. There are several explanations for this result. First, although the majority prostate epithelial cells in $Pten^{loxp/loxp};PBCre4^{+}$ mice are PTEN null, minor PTEN-positive stained cells can be detected in these mutant mice (7, 16). This may be due to the relative lower Cre activity in the basal cell compartment as a result of low AR expression (33, 34). Therefore, it is not surprising to see the existence of *Pten* heterozygous cells in the prostate cancer derived from $Pten^{loxp/loxp};PBCre4^{+}$. Secondly, *in vitro* spontaneous immortalization methods may preferentially enrich certain types of prostate cells. Primary mouse epithelial cell lines derived from genetically engineered mouse prostate cancer models including TRAMP-C1 (35), Myc-CaP (15), and our established lines here all share similar expression of PSCA, a marker for transient amplified cell population (20). Luminal cells with higher AR and probasin expressions and complete PTEN deletion may be selected out during this long-term establishment procedure. Thirdly, the *Cre* gene expression was silenced in part due to the feedback loop of PTEN-NKX-AR that can shutdown probasin promoter activity after *Pten* deletion (ref. 16; see Supplementary Fig. S1*A*).

HRPC development is a complex process including clonal selection and adaptation (3). It has been postulated that the failure of androgen ablation therapy and development of HRPC might be due to a subpopulation of androgen-independent tumor cells being present even before therapy was initiated (36). Indeed, *Nkx3.1; Pten* mutant mice can develop androgen-independent phenotypes well before they display overt PIN or cancer phenotypes (37). Because we can successfully isolate androgen-independent primary cell lines from a primary prostate tumor that has never been exposed to hormonal ablation, our study further supports this hypothesis that acquisition of androgen independence can be uncoupled from hormone deprivation pressure and selection (37).

With recent evidence suggesting that loss of PTEN is associated with progression to HRPC (28, 37, 38), our study further underscores the critical role of PTEN in HRPC development. We showed that complete loss of PTEN causes decreased p27 and E-cadherin expression, which may contribute to the enhanced gain of transformation ability in PTEN-CaP2 and PTEN-CaP8. Significantly, knockdown of PTEN in Myc-CaP cells is sufficient to change its androgen dependency. Collectively, our study showed that PTEN can functionally control "two" hits: cell transformation and androgen-independent growth in the course of HRPC tumor development.

Mounting evidence suggests that AR plays an important role in prostate cancer progression (39–41). Although AR remains critical for cell-cycle progression in androgen-independent CWR22 (42) and LAPC4 (43), the specific role of AR in PTEN-controlled HRPC progression has not been clearly defined yet. Knocking down endogenous AR expression in PTEN-CaP2 and PTEN-CaP8 cells by shRNA abolishes androgen-independent growth *in vitro*, which in part may be due to the increased expression of cell cycle inhibitor p21 and p27 and less tumorigenicity *in vivo* in female SCID mice. Therefore, our study provides evidence that HRPC development caused by PTEN loss is androgen independent but AR dependent. Further study will be critical to ascertain whether AR is required for the onset of PIN and whether AR is essential for the acquisition of AI prostate cancer in our *Pten* prostate cancer model.

Acknowledgments

Received 11/15/2006; revised 4/2/2007; accepted 4/23/2007.

Grant support: U.S. Army Medical Research and Material Command grants W81XWH-04-1-0824 (J. Jiao) and the Prostate Cancer Foundation, DOD PC031130, National Cancer Institute UO1 CA84128-06, P50 CA092131, and RO1 CA107166 (H. Wu).

The costs of publication of this article were defrayed in part by the payment of page charges. This article must therefore be hereby marked *advertisement* in accordance with 18 U.S.C. Section 1734 solely to indicate this fact.

We thank Rachel Kim, Sherly Mosessian, Reggie Hill, and colleagues in both Wu and Sawyers laboratories for helpful comments and suggestion. We acknowledge Prof. Dr. Marileila Garcia and Margaret Skokan for their great support and advice.

References

1. Jemal A, Murray T, Samuels A, Ghafoor A, Ward E, Thun MJ. Cancer statistics, 2003. CA Cancer J Clin 2003; 53:5–26.
2. Feldman BJ, Feldman D. The development of androgen-independent prostate cancer. Nat Rev Cancer 2001; 1:34–45.
3. So A, Gleave M, Hurtado-Col A, Nelson C. Mechanisms of the development of androgen independence in prostate cancer. World J Urol 2005;23:1–9.
4. Deocampo ND, Huang H, Tindall DJ. The role of PTEN in the progression and survival of prostate cancer. Minerva Endocrinol 2003;28:145–53.
5. Cansino Alcaide JR, Martinez-Pineiro L. Molecular biology in prostate cancer. Clin Transl Oncol 2006;8: 148–52.
6. Trotman LC, Niki M, Dotan ZA, et al. Pten dose dictates cancer progression in the prostate. PLoS Biol 2003;1:E59.
7. Wang S, Gao J, Lei Q, et al. Prostate-specific deletion of the murine Pten tumor suppressor gene leads to metastatic prostate cancer. Cancer Cell 2003; 4:209–21.
8. Ma X, Ziel-van der Made AC, Autar B, et al. Targeted biallelic inactivation of Pten in the mouse prostate leads to prostate cancer accompanied by increased epithelial cell proliferation but not by reduced apoptosis. Cancer Res 2005;65:5730–9.
9. Freeman D, Lesche R, Kertesz N, et al. Genetic background controls tumor development in PTEN-deficient mice. Cancer Res 2006;66:6492–6.
10. Di Cristofano A, Pesce B, Cordon-Cardo C, Pandolfi PP. Pten is essential for embryonic development and tumour suppression. Nat Genet 1998;19: 348–55.
11. Roy-Burman P, Wu H, Powell WC, Hagenkord J, Cohen MB. Genetically defined mouse models that mimic natural aspects of human prostate cancer development. Endocr Relat Cancer 2004;11:225–54.
12. Horoszewicz JS, Leong SS, Chu TM, et al. The LNCaP cell line—a new model for studies on human prostatic carcinoma. Prog Clin Biol Res 1980;37:115–32.
13. Kaighn ME, Narayan KS, Ohnuki Y, Lechner JF, Jones LW. Establishment and characterization of a human prostatic carcinoma cell line (PC-3). Invest Urol 1979;17:16–23.
14. Stone KR, Mickey DD, Wunderli H, Mickey GH, Paulson DF. Isolation of a human prostate carcinoma cell line (DU 145). Int J Cancer 1978;21:274–81.
15. Watson PA, Ellwood-Yen K, King JC, Wongvipat J, Lebeau MM, Sawyers CL. Context-dependent hormone-refractory progression revealed through characterization of a novel murine prostate cancer cell line. Cancer Res 2005;65:11565–71.
16. Lei Q, Jiao J, Xin L, et al. NKX3.1 stabilizes p53, inhibits AKT activation, and blocks prostate cancer initiation caused by PTEN loss. Cancer Cell 2006;9:367–78.
17. Xin L, Lawson DA, Witte ON. The Sca-1 cell surface marker enriches for a prostate-regenerating cell

subpopulation that can initiate prostate tumorigenesis. Proc Natl Acad Sci U S A 2005;102:6942–7.
18. Wu X, Wu J, Huang J, et al. Generation of a prostate epithelial cell-specific Cre transgenic mouse model for tissue-specific gene ablation. Mech Dev 2001;101:61–9.
19. Magee JA, Abdulkadir SA, Milbrandt J. Haploinsufficiency at the Nkx3.1 locus. A paradigm for stochastic, dosage-sensitive gene regulation during tumor initiation. Cancer Cell 2003;3:273–83.
20. Tran CP, Lin C, Yamashiro J, Reiter RE. Prostate stem cell antigen is a marker of late intermediate prostate epithelial cells. Mol Cancer Res 2002;1:113–21.
21. Shen WH, Balajee AS, Wang J, et al. Essential role for nuclear PTEN in maintaining chromosomal integrity. Cell 2007;128:157–70.
22. Brothman AR. Cytogenetics and molecular genetics of cancer of the prostate. Am J Med Genet 2002;115:150–6.
23. Zhao JJ, Gjoerup OV, Subramanian RR, et al. Human mammary epithelial cell transformation through the activation of phosphatidylinositol 3-kinase. Cancer Cell 2003;3:483–95.
24. Boehm JS, Hession MT, Bulmer SE, Hahn WC. Transformation of human and murine fibroblasts without viral oncoproteins. Mol Cell Biol 2005;25:6464–74.
25. Stiles B, Groszer M, Wang S, Jiao J, Wu H. PTENless means more. Dev Biol 2004;273:175–84.
26. Jennbacken K, Gustavsson H, Welen K, Vallbo C, Damber JE. Prostate cancer progression into androgen independency is associated with alterations in cell adhesion and invasivity. Prostate 2006;66:1631–40.
27. Waller AS, Sharrard RM, Berthon P, Maitland NJ. Androgen receptor localisation and turnover in human prostate epithelium treated with the antiandrogen, casodex. J Mol Endocrinol 2000;24:339–51.
28. Mulholland DJ, Dedhar S, Wu H, Nelson CC. PTEN and GSK3β: key regulators of progression to androgen-independent prostate cancer. Oncogene 2006;25:329–37.
29. Pei Y, Tuschl T. On the art of identifying effective and specific siRNAs. Nat Methods 2006;3:670–6.
30. Lin X, Ruan X, Anderson MG, Nicoulaz AL, Iggo R. siRNA-mediated off-target gene silencing triggered by a 7 nt complementation. Nucleic Acids Res 2005;33:4527–35.
31. Scacheri PC, Rozenblatt-Rosen O, Caplen NJ, et al. Short interfering RNAs can induce unexpected and divergent changes in the levels of untargeted proteins in mammalian cells. Proc Natl Acad Sci U S A 2004;101:1892–7.
32. Bridge AJ, Pebernard S, Ducraux A, Nicoulaz AL, Iggo R. Induction of an interferon response by RNAi vectors in mammalian cells. Nat Genet 2003;34:263–4.
33. Bonkhoff H, Remberger K. Widespread distribution of nuclear androgen receptors in the basal cell layer of the normal and hyperplastic human prostate. Virchows Arch 1993;422:35–8.
34. Wang S, Garcia AJ, Wu M, Lawson DA, Witte ON, Wu H. Pten deletion leads to the expansion of a prostatic stem/progenitor cell subpopulation and tumor initiation. Proc Natl Acad Sci U S A 2006;103:1480–5.
35. Foster BA, Gingrich JR, Kwon ED, Maidas C, Greenberg NM. Characterization of prostatic epithelial cell lines derived from transgenic adenocarcinoma of the mouse prostate (TRAMP) model. Cancer Res 1997;57:3325–30.
36. Isaacs JT. The biology of hormone refractory prostate cancer. Why does it develop? Urol Clin North Am 1999;26:263–73.
37. Gao H, Ouyang X, Banach-Petrosky WA, Shen MM, Abate-Shen C. Emergence of androgen independence at early stages of prostate cancer progression in nkx3.1; pten mice. Cancer Res 2006;66:7929–33.
38. Bertram J, Peacock JW, Fazli L, et al. Loss of PTEN is associated with progression to androgen independence. Prostate 2006;66:895–902.
39. Balk SP. Androgen receptor as a target in androgen-independent prostate cancer. Urology 2002;60:132–8; discussion 8–9.
40. Debes JD, Tindall DJ. Mechanisms of androgen-refractory prostate cancer. N Engl J Med 2004;351:1488–90.
41. Ergun A, Lawrence CA, Kohanski MA, Brennan TA, Collins JJ. A network biology approach to prostate cancer. Mol Syst Biol 2007;3:82.
42. Yuan X, Li T, Wang H, et al. Androgen receptor remains critical for cell-cycle progression in androgen-independent CWR22 prostate cancer cells. Am J Pathol 2006;169:682–96.
43. Chen CD, Welsbie DS, Tran C, et al. Molecular determinants of resistance to antiandrogen therapy. Nat Med 2004;10:33–9.